Brief communication

MOLECULAR METABOLISM

Knockout of STAT3 in skeletal muscle does not prevent high-fat diet-induced insulin resistance

Amanda T. White [1,2], Samuel A. LaBarge [1], Carrie E. McCurdy [3], Simon Schenk [1,2,*]

ABSTRACT

Objective: Increased signal transducer and activator of transcription 3 (STAT3) signaling has been implicated in the development of skeletal muscle insulin resistance, though its contribution, *in vivo*, remains to be fully defined. Therefore, the aim of this study was to determine whether knockout of skeletal muscle STAT3 would prevent high-fat diet (HFD)-induced insulin resistance.

Methods: We used Cre-LoxP methodology to generate mice with muscle-specific knockout (KO) of STAT3 (mKO). Beginning at 10 weeks of age, mKO mice and their wildtype/floxed (WT) littermates either continued consuming a low fat, control diet (CON; 10% of calories from fat) or were switched to a HFD (60% of calories from fat) for 20 days. We measured body composition, energy expenditure, oral glucose tolerance and *in vivo* insulin action using hyperinsulinemic-euglycemic clamps. We also measured insulin sensitivity in isolated *soleus* and *extensor digitorum longus* muscles using the 2-deoxy-glucose (2DOG) uptake technique.

Results: STAT3 protein expression was reduced ~75–100% in muscle from mKO vs. WT mice. Fat mass and body fat percentage did not differ between WT and mKO mice on CON and were increased equally by HFD. There were also no genotype differences in energy expenditure or whole-body fat oxidation. As determined, *in vivo* (hyperinsulinemic-euglycemic clamps) and *ex vivo* (2DOG uptake), skeletal muscle insulin sensitivity did not differ between CON-fed mice, and was impaired similarly by HFD.

Conclusions: These results demonstrate that STAT3 activation does not underlie the development of HFD-induced skeletal muscle insulin resistance.

Keywords In vivo; STAT3; Glucose homeostasis; Clamp; Obesity; Cre-LoxP

1. INTRODUCTION

Insulin resistance is a common metabolic defect in obesity that is implicated in the pathogenesis of type 2 diabetes [1,2]. Mechanistically, various cytokines secreted from obese adipose tissue, such as leptin, adiponectin, tumor necrosis factor α (TNFα) and interleukin 6 (IL-6) have been shown to modulate peripheral insulin action [1,2]. Cytokine-mediated crosstalk with peripheral tissues occurs through janus kinase (JAK)-signal transducer and activator of transcription (STAT), particularly STAT3, signaling [3–6]. Specifically, interaction of cytokines with a membrane receptor leads to activation of JAK, which then phosphorylates cytosolic STAT3 at a key tyrosine residue (Y705) required for STAT3 dimerization and nuclear translocation [4–6]. Nuclear STAT3 affects the transcription of various target genes, including suppressor of cytokine signaling 3 (SOCS3) [5,6]. This is important as SOCS3 can negatively regulate insulin signaling through interactions with the insulin receptor (IR) and IR substrate (IRS) proteins, and, as a result, elevated STAT3 signaling has been implicated in obesity-induced insulin resistance [3–6].

Skeletal muscle is an important tissue for post-prandial systemic glucose disposal [7], and interventions that prevent or reverse skeletal muscle insulin resistance in the face of obesity hold promise for the prevention and/or treatment of type 2 diabetes (T2D). Supporting a role for STAT3 in the pathogenesis of skeletal muscle insulin resistance in obesity and T2D, phosphorylated (p)-STAT3 is increased in skeletal muscle from patients with impaired glucose tolerance (IGT) or T2D [8,9]. Moreover, prolonged palmitate treatment of L6 myotubes *in vitro* (which mimics the high fatty acid levels observed in obesity) led to constitutive STAT3 activation, increased SOCS3 protein abundance and impaired insulin-stimulated Akt signaling [9]. Importantly, STAT3 knockdown attenuated these palmitate-induced impairments in insulin signaling [9], as well as insulin resistance caused by chronic treatment of human skeletal muscle myoblasts (HSMM) with IL-6 [8]. In fact, STAT3 silencing in L6 myotubes not only prevented palmitate-mediated insulin

[1]Department of Orthopaedic Surgery, University of California San Diego, La Jolla, CA, USA [2]Biomedical Sciences Graduate Program, University of California San Diego, La Jolla, CA, USA [3]Department of Human Physiology, University of Oregon, Eugene, OR, USA

*Corresponding author. Department of Orthopaedic Surgery, School of Medicine, University of California San Diego, 9500 Gilman Drive MC0863, La Jolla, CA 92093, USA. Tel.: +1 858 822 0857; fax: +1 858 822 3807. E-mail: sschenk@ucsd.edu (S. Schenk).

Abbreviations: 2DOG, 2-deoxyglucose; *Adgre1*, adhesion G protein-coupled receptor E1; AT, adipose tissue; CON, normal chow, control diet; EDL, extensor digitorum longus; GA, gastrocnemius; GIR, glucose infusion rate; HFD, high-fat diet; HGP, hepatic glucose production; HYP-EUG, hyperinsulinemic-euglycemic; IL, interleukin; IS-GDR, insulin-stimulated glucose disposal rate; KO, knockout; MCK, muscle creatine kinase; mKO, muscle-specific knockout of STAT3; STAT3, signal transducer and activator of transcription 3; T2D, type 2 diabetes; WT, wild-type

Received March 10, 2015 • Revision received April 29, 2015 • Accepted May 5, 2015 • Available online 13 May 2015

http://dx.doi.org/10.1016/j.molmet.2015.05.001

resistance but also enhanced insulin-stimulated glycogen synthesis in both control- and palmitate-treated cells [9]. Similarly, mice with knockout (KO) of SOCS3 in skeletal muscle are refractory to HFD-induced insulin resistance [10]. Taken together, these studies identify increased STAT3 activation as a possible underlying mechanism of skeletal muscle insulin resistance in obesity and highlight the potential of STAT3 inhibition for the treatment of insulin resistance and type 2 diabetes. Notably, however, to date mechanistic studies have only been performed in muscle cells, *in vitro*, so whether these findings translate *in vivo* remains to be elucidated. Thus, to address the role of STAT3 in modulating skeletal muscle insulin action, we used Cre-LoxP methodology in this study to generate mice with muscle-specific KO of STAT3 (mKO). Our goal was to determine whether knocking out STAT3 would enhance skeletal muscle insulin sensitivity and whether it would protect against HFD-induced insulin resistance.

2. METHODS

2.1. Animals

The mKO mice were generated by crossing mice with loxP sites flanking exon 22 of the STAT3 gene [11,12] (kindly provided by Dr. Michael Karin, UC San Diego, and used with permission of Dr. Shizuo Akira, Osaka University) with mice expressing Cre recombinase under the control of the muscle creatine kinase (MCK) promoter. In this model, an essential acetylation (K685) and phosphorylation site (Y705), which are necessary for STAT3 activation, are deleted [11–13]. The control/wildtype (WT) mice for all studies were floxed, Cre-negative littermates, and all studies were conducted in male mice. Major endpoint measurements, including *ex vivo* insulin-stimulated 2-deoxyglucose glucose (2DOG) uptake, hyperinsulinemic-euglycemic (HYP-EUG) clamps, oral glucose tolerance tests (OGTT), were performed in fasted (4–6 h), 13 week old mice between 1230 and 1500 h. All tissues and blood were excised from fasted, anesthetized mice undergoing assessment of 2DOG uptake. These tissues were immediately rinsed in saline, and frozen in liquid nitrogen. All experiments were approved by and conducted in accordance with the Animal Care Program at the University of California, San Diego.

2.2. Diet

At 10 weeks of age, mice were randomized to either continue control (10% calories from fat) diet (CON) or were switched to a high-fat diet (HFD; 60% calories from fat. Cat#D12492, Research Diets, New Brunswick, NJ) for 20 days. Importantly, previous studies have demonstrated that this duration (or less) of HFD increases fat mass and causes systemic and adipose tissue inflammation and/or impaired whole body and skeletal muscle insulin sensitivity [14–17]. To confirm that our model resulted in systemic ($n = 4–8$/group) and adipose tissue ($n = 4$/group) inflammation, in a preliminary experiment, we placed WT mice on CON or HFD for 5 days or 3 weeks. After just 5 days, plasma IL-6 was increased ~8-fold (CON: 1.1 ± 0.1, HFD: 9.1 ± 2.3 pg/mL, $P < 0.05$, $n = 4–8$/group), and after 3 weeks adhesion G protein-coupled receptor E1 (*Adgre1*; referred to as F4/80) and *Cd68* gene expression were increased in HFD vs. CON by 42% and 64%, respectively (F4/80 — CON: 1.00 ± 0.09, HFD: 1.64 ± 0.23, $P < 0.05$; *Cd68* — CON: 1.00 ± 0.08, HFD: 1.42 ± 0.09, $P < 0.05$). Together this verifies that our model results in both systemic and adipose tissue inflammation.

2.3. Single myofiber isolation

Excised *tibialis anterior* was placed in 0.9% saline and cleaned of visible fascia, tendon, and fat using a Leica EZ4 dissection microscope (Leica Microsystems, Germany). Individual myofibers were mechanically separated using forceps, and approximately 25 myofibers were placed directly into 1X Laemmli sample buffer (LSB), boiled for 5 min at 100 °C, and frozen at −80 °C for immunoblotting analysis.

2.4. 2DOG uptake

Basal and insulin-stimulated (0.36 nmol/L) 2DOG uptake was measured in isolated, paired *soleus* and *extensor digitorum longus* (EDL) muscles as previously described [18–20].

2.5. *In vivo* IL-6 injection

In anaesthetized WT and mKO mice, one *gastrocnemius* (GA) was dissected and the inferior vena cava was exposed. Mice were then injected with 55 μg/kg of IL-6 (rM-IL-6, Cat#200–02, Shenandoah Biotechnology), in order to activate STAT3. At 10 min after the IL-6 injection, the contralateral GA was dissected. Immediately after dissection, the GA muscles were rinsed in saline, blotted dry and frozen in liquid nitrogen for subsequent analysis.

2.6. Immunoblotting

Tissues were homogenized and immunoblotting was performed by SDS-PAGE, as described previously [18–20]. The following antibodies were used: STAT3 (Cat# 9132) and phosphorylated STAT3 (pSTAT3: Cat# 9138) from Cell Signaling Technology; glyceraldehyde-3-phosphate dehydrogenase (GAPDH; 10R-G109a) from Fitzgerald Industries and actin (sc-10731) from Santa Cruz Biotechnology. Nuclear and cytosolic fractions were isolated using a commercially available kit (78835: NE-PER; Thermo Scientific) with the addition of the COMPLETE protease inhibitor mixture (11697498001; Roche Applied Science).

2.7. Oral glucose tolerance test (OGTT)

After 15–17 days on diet, 4 h-fasted mice were orally gavaged with 5 g/kg dextrose. Blood glucose concentration was measured by tail vein at 0, 20, 40, 60, 80 and 120 min after gavage.

2.8. Hyperinsulinemic-euglycemic (HYP-EUG) clamps

Studies were conducted in chronically cannulated, conscious, fasted (6 h) mice as previously described [18]. During the clamp, insulin (Humulin R, Eli Lilly and Company) was infused at a rate of 4 mU/kg/min. [3-^{3}H] D-glucose (5 Ci/h; PerkinElmer) was co-infused for calculation of hepatic glucose production (HGP) and glucose disposal. The insulin-stimulated glucose disposal rate (IS-GDR; glucose disposal during clamp minus basal glucose disposal) was used as an index of skeletal muscle insulin sensitivity. Blood glucose concentration was clamped at 125 mg/dL.

2.9. Energy expenditure and body composition

Energy expenditure (EE), respiratory exchange ratio (RER), and spontaneous activity were measured by the CLAMS system, and body composition was assessed by magnetic resonance imaging, as described previously [19,20]. All measurements were made ~18 days after the start of dietary intervention.

2.10. Plasma hormone concentrations

Leptin, IL-6 and resistin were assessed using the Milliplex mouse adipokine assay (Millipore, Billerica, MA), and insulin was measured by ELISA (Alpco Diagnostics). For this analysis, whole blood was collected from the inferior vena cava of fasted, anesthetized mice, placed in a tube with EDTA, and centrifuged at 5,000 g at 4 °C for 5 min. The plasma was frozen at −80 °C for subsequent analysis.

2.11. PCR and qPCR

To validate excision of exon 22 in the mKO, genomic DNA was isolated from skeletal muscle (soleus, EDL and *gastrocnemius* [GA]), epididymal adipose tissue and liver. A standard PCR protocol was then used on a Bio-Rad MyCycler thermal cycler and products were run on a 2% agarose gel and visualized. The primers used have been described by others [11]. qPCR analysis was conducted, using *Gapdh* as a housekeeping gene, as previously described [18–20]. Primers used were: *Cd68* 5′-ACCGCTTATAGCCCAAGGAACAGA-3′ and 3′-AAGTGCTACTGTGGATGTCGGTGT-5'; *Adgre1* (adhesion G protein-coupled receptor E1; referred to as F4/80) 5′-CTCAAGGACACGAGGTTGCT-3′ and 3′-AGTGACAGACGAGTTGGCAG-5'.

2.12. Statistics

Statistical analyses were performed using SPSS, with significance set at $p < 0.05$. Data were analyzed by two or three-way ANOVA with repeated measures when necessary, followed by Tukey's post-hoc analysis. For HGP and the 2DOG uptake, main effects were diet, genotype, and treatment (basal vs. insulin). Once a significant effect for treatment was found, data were separated and a two-way ANOVA within basal and within insulin/clamp was performed. For EE data, a three-way ANOVA was performed for the main effects diet, genotype, and time (light vs. dark). Where there was a significant effect of time, data were analyzed by two-way ANOVA within light and within dark. STAT3 protein abundance, plasma hormone concentrations, OGTT AUC, GIR, IS-GDR, percent suppression of HGP and blood glucose during the final 30 min of the HYP-EUG clamp were analyzed by two-way ANOVA followed by Tukey's post-hoc analysis, where applicable. For the OGTT, a two-way ANOVA (diet and genotype) was used to compare blood glucose levels within each time point, followed by Tukey's post-hoc analysis. For non-diet-based comparisons between WT and mKO mice (e.g., STAT3 abundance, pSTAT3, gene expression), an unpaired t-test was used. All data are expressed as mean ± SEM.

3. RESULTS

3.1. Mouse model

Measurements in genomic DNA demonstrate that exon 22 of the STAT3 gene was efficiently deleted in various skeletal muscles of mKO vs. WT mice, but this deletion did not occur in liver or epididymal fat (Figure 1A). These genomic DNA data are complimented by muscle-specific knockdown (~75%) of STAT3 protein in whole-cell lysate from mKO vs. WT mice (Figure 1B). One issue with assessing STAT3 abundance in whole muscle is that there are a number of different cell types, other than mature myofibers, that make up skeletal muscle. Accordingly, to confirm STAT3 was knocked out in mature myofibers, we measured STAT3 in isolated myofibers, which demonstrated essentially ~100% knockdown of STAT3 (Figure 1C). In addition, to verify functional KO of STAT3 in mKO mice, we measured *in vivo* activation of STAT3 in response to IL-6. Importantly, while IL-6 stimulation increased pSTAT3 in WT mice by ~6-fold, in mKO mice there was no induction of pSTAT3 (Figure 1D). Complementing the single fiber studies, there was ~90% knockdown of total STAT3 protein in the cytosolic and nuclear fractions, with no effect of diet in these fractions (Figure 1D). Altogether, these data validate that STAT3 signaling was significantly reduced in mKO vs. WT muscle and supports the use of the mKO mouse to study the role of STAT3 in the regulation of muscle insulin action with HFD feeding.

3.2. Body mass and energy expenditure

Fat mass and percent body fat were significantly increased after 20 days of HFD feeding in both WT and mKO mice, although there was no effect on total body weight (Figure 2A–B). In line with these data, epididymal fat pad mass was significantly higher in HFD-fed mice, but there was no effect of diet or genotype on *gastrocnemius* or *tibialis anterior* muscle mass, liver mass, or heart mass (Table 1). Caloric intake was increased for both WT and mKO mice on HFD, largely resulting from increased feeding during the light phase (Figure 2C). Spontaneous activity, as measured by all beam breaks on the x-axis (x-total), was increased during the dark phase as compared with the light phase but was not significantly affected by genotype or diet (Figure 2D). $\dot{V}O_2$ was higher during the dark vs. the light phase but was unaffected by diet or genotype (Figure 2E). RER was decreased equally by HFD, as compared with CON, in both WT and mKO mice (Figure 2F).

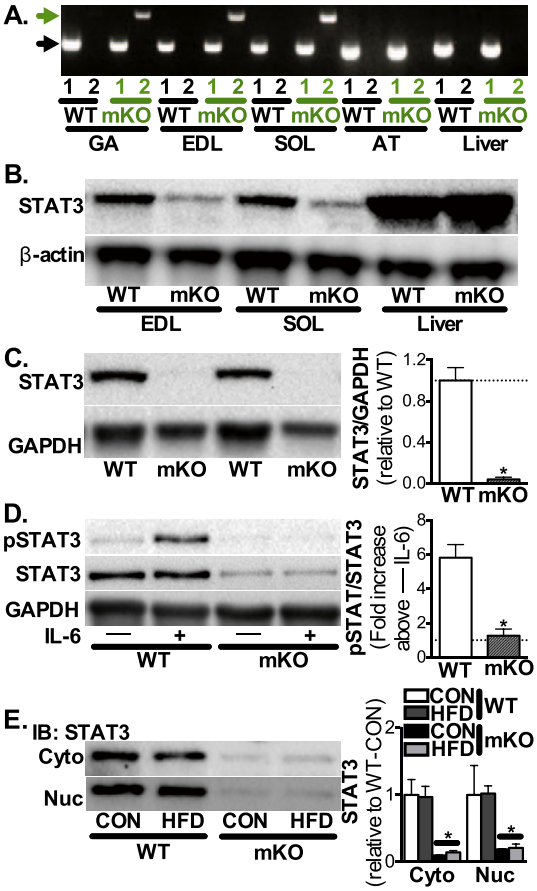

Figure 1: mKO mice have decreased STAT3 protein expression in skeletal muscle: (A) PCR on genomic DNA from skeletal muscle (*gastrocnemius* [GA], *soleus* [SOL] and *extensor digitorum longus* [EDL]), adipose tissue (AT) and liver of WT and mKO (mKO) mice. Primers target a region within exon 20 of the STAT3 gene (Lane #1), which is present in all tissues (black arrow), or a region that spans exons 20–22 (Lane #2) and thus only prime when the floxed region is deleted (green arrow, note: band only in skeletal muscle from mKO mice). (B) Total STAT3 protein abundance measured in whole-cell lysates (WCL) of SOL, EDL and liver from WT and mKO mice. (C) Total STAT3 protein abundance in myofibers isolated from the *tibialis anterior*. (D) Activation of STAT3, as measured by pSTAT3, in WCL from gastrocnemius from mice before (−) and 10 min after (+) intravenous injection with IL-6 (55 μg/kg). (E) Total STAT3 protein abundance in nuclear (nuc) and cytosolic (cyto) fractions of GA muscle.

3.3. Plasma hormone concentrations and oral glucose tolerance

HFD increased plasma leptin and resistin concentrations were increased by ~2–3 fold and ~70–130%, respectively, with no difference between genotypes (Table 2). While fasting blood glucose concentrations were not different between groups (Figure 3A), HFD

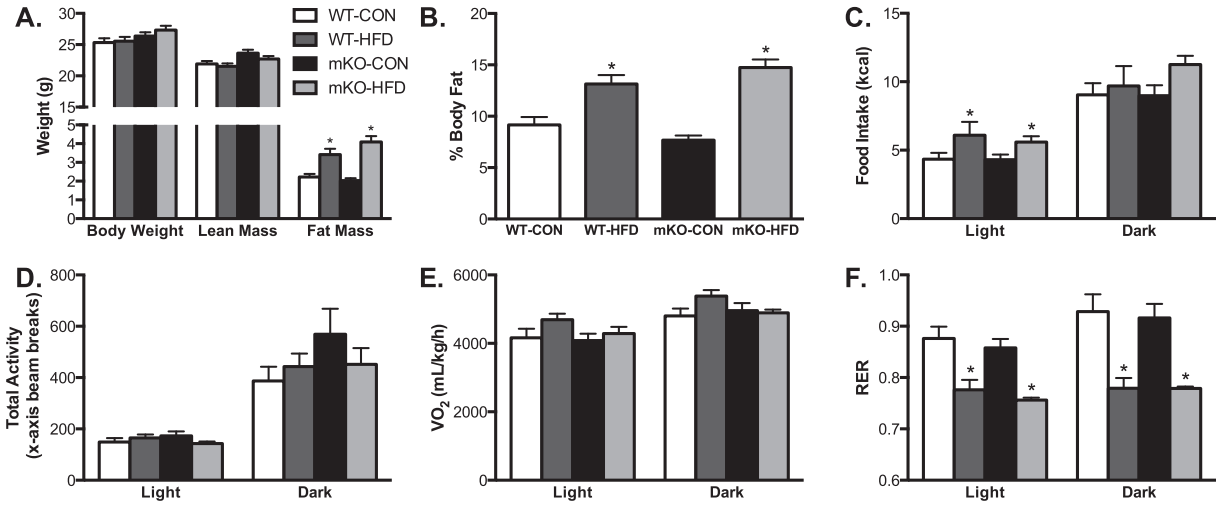

Figure 2: HFD feeding increases body fat and decreases respiratory exchange ratio (RER) in WT and mKO mice. WT and mKO mice were fed a CON or HFD for 20 d. (A) Body mass, lean mass, fat mass, and (B) percent body fat, as measured by MRI. n = 14–23/group. *, $p < 0.05$ vs. CON. (C–F) Food intake, energy expenditure, and spontaneous activity measurements were made using the CLAMS system over 3 consecutive days and averages for the light and dark cycles on days 2 and 3 are presented. (C) Cumulative food intake. (D) Total (x-total) activity was measured as all beam breaks on the horizontal axis. (E) $\dot{V}O_2$ and (F) RER were measured by indirect calorimetry. n = 6/group. *, $p < 0.05$ vs. CON. Data reported as mean ± SEM.

feeding did cause fasting hyperinsulinemia (Table 2). Blood glucose concentrations during an OGTT were significantly higher in HFD-vs. CON-fed mice, but there was no effect of genotype (Figure 3A). Accordingly, the area under the curve for the OGTT was ~30% higher in HFD-fed vs. CON-fed mice (WT-CON: 23032 ± 789, WT-HFD: 28187 ± 786, mKO-CON: 21528 ± 814, mKO-HFD: 27442 ± 1144 mg min/dL, $p < 0.05$, n = 6–10/group).

3.4. HYP-EUG clamps

In support of the OGTT data, the glucose infusion rate (GIR) during a HYP-EUG clamp was impaired ~40% in HFD-vs. control-fed mice. (Figure 3C). This impairment was due to reduced liver and skeletal muscle insulin sensitivity. Thus, HGP during the clamp was higher in HFD mice (Figure 3D), resulting in a 35–45% lower percentage suppression of hepatic glucose production during the clamp (Figure 3E). In addition, while skeletal muscle insulin sensitivity, as measured by the IS-GDR, was reduced by ~40% in WT-HFD mice, this reduction was not prevented in mKO mice. Average blood glucose concentration during the final 30 min of the clamp was not different between groups (WT-CON: 124 ± 2, WT-HFD: 128 ± 2, mKO-CON: 127 ± 1, mKO-HFD: 125 ± 1 mg/dL, $P > 0.05$).

3.5. Skeletal muscle insulin sensitivity

Basal and insulin 2DOG uptake was decreased similarly by HFD as compared to CON in both WT and mKO mice in *soleus* (Figure 4A) and EDL muscles (Figure 4B). Similar to *in vivo* findings from the HYP-EUG clamp, insulin-stimulated 2DOG uptake (i.e., insulin 2DOG − basal 2DOG) in *soleus* and EDL muscles did not differ between WT and mKO mice on CON diet (Figure 4C). Moreover, insulin-stimulated 2DOG uptake was significantly decreased by HFD as compared to CON, but there was no effect of STAT3 knockout on this impairment (Figure 4C).

4. DISCUSSION

STAT3 has been proposed to be a regulator of insulin resistance in obese and insulin-resistant states largely due to the fact that it is activated by adipocytokines, such as IL-6 and leptin, which are increased by nutrient overload and inflammation, [3–6]. Herein, we generated mice with muscle-specific knockout of STAT3 in order to investigate the mechanistic role of STAT3 in the pathophysiology of skeletal muscle insulin resistance *in vivo*. Interestingly, our results demonstrate that knockout of STAT3 does not enhance skeletal muscle insulin sensitivity in CON-fed mice, nor does it prevent HFD-induced impairments in glucose tolerance or insulin sensitivity.

Constitutive STAT3 activation has been implicated in the etiology of skeletal muscle insulin resistance. Phosphorylated STAT3 (pSTAT3), which is a marker of its activation, is increased in skeletal muscle from patients with impaired glucose tolerance and T2D as compared to healthy controls [8,9]. In mice, IL-6 infusion impairs activation of insulin signaling and skeletal muscle glucose uptake during a HYP-EUG clamp [21]. In L6 myotubes, palmitate treatment, which is used to mimic the high fatty acid levels common to obesity and T2D, increases STAT3 activation and reduces insulin-stimulated Akt activation and glycogen

Table 1 – Tissue mass (mg).

	WT-CON	WT-HFD	mKO-CON	mKO-HFD
Gastrocnemius	120 ± 3	123 ± 3	123 ± 3	122 ± 4
Tibialis anterior	43 ± 1	45 ± 1	45 ± 1	45 ± 1
Epididymal fat	327 ± 25	527 ± 41*	288 ± 17	621 ± 51*
Liver	1,192 ± 37	1,011 ± 32	1,170 ± 57	1,066 ± 30
Heart	122 ± 3	132 ± 4	126 ± 3	136 ± 4

Tissues were weighed to the nearest mg. n = 19–24/group. *, $p < 0.05$ vs. control (CON) diet.
Data reported as mean ± SEM.

Table 2 – Plasma concentrations (pg/mL).

	WT-CON	WT-HFD	mKO-CON	mKO-HFD
Leptin	1351 ± 436	4182 ± 1003*	938 ± 164	3974 ± 699*
Resistin	2003 ± 94	3380 ± 254*	1481 ± 223	3382 ± 427*
Insulin	496 ± 128	1,094 ± 122*	672 ± 112	1,159 ± 142*

n = 4–11/group. *, $p < 0.05$ vs. control (CON) diet. Data reported as mean ± SEM.

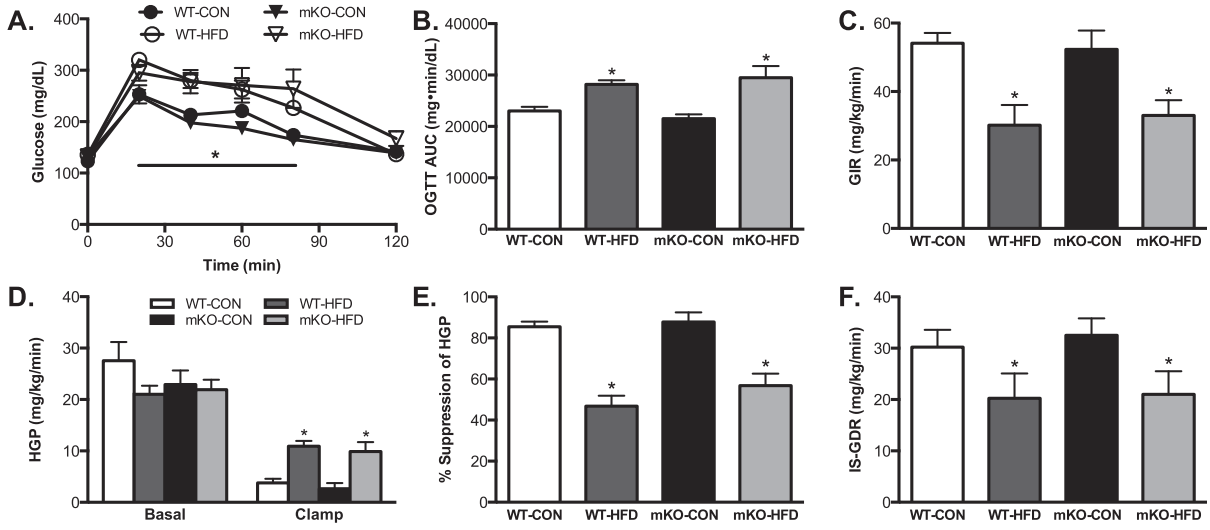

Figure 3: HFD-induced impairments in glucose tolerance or *in vivo* insulin action are similar in mKO and WT mice. WT and mKO mice were fed a CON or HFD for 20 days. (A) Blood glucose concentrations and (B) area under the curve (AUC) during an oral glucose tolerance test (OGTT; 5 g/kg). n = 6–15/group. *, $p < 0.05$ vs. CON. (C) Glucose infusion rate (GIR), (D) hepatic glucose production (HGP; basal and insulin-stimulated [clamp]), (E) percent suppression of HGP, and (F) insulin-stimulated glucose disposal rate (IS-GDR) during a HYP-EUG clamp. n = 7–10/group. *, $p < 0.05$ vs. CON. Data reported as mean ± SEM.

synthesis [9]. This effect is STAT3-dependent, as siRNA against STAT3 attenuated these changes [9]. Similarly, in human skeletal muscle myoblasts, impaired Akt signaling and insulin-stimulated glucose uptake resulting from IL-6 treatment is reversed by STAT3 siRNA treatment [8]. Interestingly, STAT3 knockdown in control-treated L6 myotubes [9], but not in cultured human muscle myotubes [8], also improved insulin-mediated Akt activation and glycogen synthesis. While these studies suggest a causative role for STAT3 in skeletal muscle insulin resistance, this perspective is not universal. For example, STAT3 activation by IL-6 treatment did not reduce insulin stimulation of Akt-AS160 in human skeletal muscle strips [22] or insulin signaling or GLUT4 translocation and glucose uptake in L6 myotubes [23]. In fact, treatment of C2C12 myotubes with a selective alpha-7 nicotinic receptor agonist, PNU-282987, increases insulin-stimulated glucose uptake in a STAT3-dependent manner [24]. Moreover, reduced IL-6-induced activation of STAT3 in skeletal muscle cells from T2D subjects is thought to contribute to impaired insulin sensitivity in these patients, rather than cause their insulin resistance [25]. From these studies it is clear that there is debate as to whether STAT3 plays a causative role in skeletal muscle insulin resistance, which in the present study we sought to clarify by studying the mKO mouse. From our results it can be concluded that STAT3 is not a significant contributor to skeletal muscle insulin sensitivity in CON-fed mice, and that it does not contribute to the pathogenesis of insulin resistance caused by 3 weeks of HFD feeding.

Increased body weight, fat mass, and percent body fat have been observed in mice with constitutive activation of STAT3 in POMC neurons along with increased food intake [26], suggesting that modulation of STAT3 activity may alter whole body energy metabolism. However, the effects of STAT3 modulation in neurons may reflect the central role of STAT3 (e.g., in leptin signaling [27]), and peripheral STAT3 may play a separate role in energy homeostasis. For example, aP2-driven knockout of STAT3 in adipose tissue did not alter food intake or energy expenditure, but increased body weight and adiposity in this model were noted and thought to be due to impairments in leptin signaling [28]. In the present study, we observed no differences in body weight, fat mass, percent body fat, or food intake in mKO vs. WT mice on CON, and HFD increased these parameters equally for both genotypes with no overall increase in body weight. Considering the emerging role of STAT3 in mitochondrial bioenergetics [29–32], we thought it possible that modulation of STAT3 in skeletal muscle could impact whole body energy metabolism. However, we did not observe any effects of muscle-specific STAT3 knockout on $\dot{V}O_2$ or RER, suggesting that skeletal muscle STAT3 is not a major regulator of whole body energy homeostasis.

Despite the potential of STAT3 inhibition to ameliorate insulin resistance in cell models [8,9,33], STAT3 has been implicated as a positive mediator of glucose homeostasis through inhibition of gluconeogenic genes in the liver [24,34–36]. For example, STAT3 knockout in the

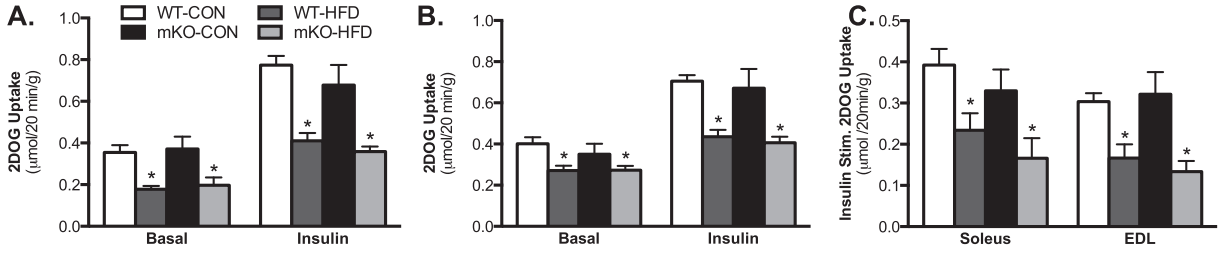

Figure 4: STAT3 knockout in muscle does not protect against HFD-induced impairments in skeletal muscle insulin sensitivity. WT and mKO mice were fed a CON or HFD for 20 days. Basal and insulin (60 μU/mL) 2-deoxyglucose (2DOG) uptake in paired (A) soleus and (B) EDL muscles. (C) Insulin-stimulated 2DOGU (calculated as insulin 2DOG uptake − basal 2DOG uptake) in isolated soleus and EDL muscles. n = 6–15/group. *, $p < 0.05$ vs. CON. Data reported as mean ± SEM.

liver increases blood glucose and plasma insulin concentrations and impairs glucose tolerance [24,34,35]. Similarly, combined knockout of STAT3 in the hypothalamus and pancreatic β cells increases body weight, plasma glucose and insulin concentrations, and impairs glucose tolerance [37]. In contrast, we found no effect of STAT3 on blood glucose concentration, glucose tolerance or body weight. Taken together, these results suggest that the role of STAT3 in the modulation of whole-body glucose homeostasis is tissue-specific, and that skeletal muscle STAT3 is not an important contributor.

A possible limitation of our study is that our HFD feeding protocol was for 3 weeks and may not have been sufficient to induce overt inflammation. However, we found that up to 3 weeks HFD increased % body fat, epididymal fat mass, adipose tissue (i.e., F4/80 and *Cd68*) and systemic markers of inflammation (i.e., resistin, IL-6). This is in line with previous studies that found that as little as 3 days [14,16,17] of HFD, and certainly 1–3 weeks, increases pro-inflammatory macrophage infiltration of epididymal fat as measured by flow cytometry and gene expression analysis [14,38]. However, in a recent study, gene expression markers of inflammation were not increased after 3 weeks of HFD despite impairments in muscle insulin action [15]. Furthermore, the ~33–50% impairment of skeletal muscle insulin sensitivity that we observed is comparable to previous studies using a 3 week HFD model [14,15]. Thus, overall, we are confident that our model appropriately addresses the contribution of skeletal muscle STAT3 to HFD- and inflammation-induced insulin resistance.

5. CONCLUSION

In conclusion, we investigated whether muscle-specific knockout of STAT3 enhances insulin sensitivity, whole body energy homeostasis, or glucose tolerance. As inhibition of STAT3 activity has been observed to reverse the detrimental effects of palmitate and cytokines on insulin signaling, we employed a HFD mouse model to determine whether muscle-specific STAT3 knockout prevents HFD-induced insulin resistance. Overall, we found that knockout of STAT3 in skeletal muscle does not improve sensitivity in CON-fed mice or ameliorate the detrimental effects of HFD feeding on insulin sensitivity, glucose tolerance, or body composition. Thus, inhibition of skeletal muscle STAT3 does not appear to be a promising approach for modulating skeletal muscle insulin action.

CONFLICT OF INTEREST

None declared.

AUTHOR CONTRIBUTIONS

S.S. and A.T.W. were responsible for the conception and design of the study, and the analysis and interpretation of data. A.T.W was responsible for the design and drafting of the manuscript and S.S. revised the manuscript critically. S.L. and C.E.M. contributed to analysis, interpretation of data and critical revision of the manuscript. All authors gave final approval.

ACKNOWLEDGMENTS

The authors are grateful to Benjamin Huang for assistance with mouse studies. We also thank the UC San Diego Animal Care Program Phenotyping Core for CLAMS measurements and Dr. Jianhua Shao (Department of Pediatrics, University of California, San Diego, CA, USA) for use of the MRI machine. This research was funded in part by the National Institutes of Health (NIH) grants R01 AG043120, P30 AR061303, P30 AR058878, P30 DK063491, R24 HD050837 and R01 DK095926, and a Post-Doctoral Fellowship (for S.A.L.) from the Frontiers of Innovation Scholars Program at UC San Diego.

REFERENCES

[1] Osborn, O., Olefsky, J.M., 2012. The cellular and signaling networks linking the immune system and metabolism in disease. Nature Medicine 18:363–374.
[2] Schenk, S., Saberi, M., Olefsky, J.M., 2008. Insulin sensitivity: modulation by nutrients and inflammation. Journal of Clinical Investigation 118:2992–3002.
[3] Du, Y., Wei, T., 2014. Inputs and outputs of insulin receptor. Protein & Cell 5: 203–213.
[4] Galic, S., Sachithanandan, N., Kay, T.W., Steinberg, G.R., 2014. Suppressor of cytokine signalling (SOCS) proteins as guardians of inflammatory responses critical for regulating insulin sensitivity. Biochemical Journal 461:177–188.
[5] Kristiansen, O.P., Mandrup-Poulsen, T., 2005. Interleukin-6 and diabetes: the good, the bad, or the indifferent? Diabetes 54(Suppl 2):S114–S124.
[6] Wunderlich, C.M., Hovelmeyer, N., Wunderlich, F.T., 2013. Mechanisms of chronic JAK-STAT3-SOCS3 signaling in obesity. JAK-STAT 2:e23878.
[7] DeFronzo, R.A., Tripathy, D., 2009. Skeletal muscle insulin resistance is the primary defect in type 2 diabetes. Diabetes Care 32(Suppl 2):S157–S163.
[8] Kim, T.H., Choi, S.E., Ha, E.S., Jung, J.G., Han, S.J., Kim, H.J., et al., 2013. IL-6 induction of TLR-4 gene expression via STAT3 has an effect on insulin resistance in human skeletal muscle. Acta Diabetologica 50:189–200.
[9] Mashili, F., Chibalin, A.V., Krook, A., Zierath, J.R., 2013. Constitutive STAT3 phosphorylation contributes to skeletal muscle insulin resistance in type 2 diabetes. Diabetes 62:457–465.
[10] Jorgensen, S.B., O'Neill, H.M., Sylow, L., Honeyman, J., Hewitt, K.A., Palanivel, R., et al., 2013. Deletion of skeletal muscle SOCS3 prevents insulin resistance in obesity. Diabetes 62:56–64.
[11] Takeda, K., Clausen, B.E., Kaisho, T., Tsujimura, T., Terada, N., Forster, I., et al., 1999. Enhanced Th1 activity and development of chronic enterocolitis in mice devoid of Stat3 in macrophages and neutrophils. Immunity 10:39–49.
[12] Takeda, K., Kaisho, T., Yoshida, N., Takeda, J., Kishimoto, T., Akira, S., 1998. Stat3 activation is responsible for IL-6-dependent T cell proliferation through preventing apoptosis: generation and characterization of T cell-specific Stat3-deficient mice. Journal of Immunology 161:4652–4660.
[13] Nie, Y., Erion, D.M., Yuan, Z., Dietrich, M., Shulman, G.I., Horvath, T.L., et al., 2009. STAT3 inhibition of gluconeogenesis is downregulated by SirT1. Nature Cell Biology 11:492–500.
[14] Lee, Y.S., Li, P., Huh, J.Y., Hwang, I.J., Lu, M., Kim, J.I., et al., 2011. Inflammation is necessary for long-term but not short-term high-fat diet-induced insulin resistance. Diabetes 60:2474–2483.
[15] Turner, N., Kowalski, G.M., Leslie, S.J., Risis, S., Yang, C., Lee-Young, R.S., et al., 2013. Distinct patterns of tissue-specific lipid accumulation during the induction of insulin resistance in mice by high-fat feeding. Diabetologia 56:1638–1648.
[16] Elgazar-Carmon, V., Rudich, A., Hadad, N., Levy, R., 2008. Neutrophils transiently infiltrate intra-abdominal fat early in the course of high-fat feeding. Journal of Lipid Research 49:1894–1903.
[17] Talukdar, S., Oh, D.Y., Bandyopadhyay, G., Li, D., Xu, J., McNelis, J., et al., 2012. Neutrophils mediate insulin resistance in mice fed a high-fat diet through secreted elastase. Nature Medicine 18:1407–1412.
[18] Schenk, S., McCurdy, C.E., Philp, A., Chen, M.Z., Holliday, M.J., Bandyopadhyay, G.K., et al., 2011. Sirt1 enhances skeletal muscle insulin sensitivity in mice during caloric restriction. Journal of Clinical Investigation 121:4281–4288.
[19] White, A.T., McCurdy, C.E., Philp, A., Hamilton, D.L., Johnson, C.D., Schenk, S., 2013. Skeletal muscle-specific overexpression of SIRT1 does not enhance whole-body energy expenditure or insulin sensitivity in young mice. Diabetologia 56:1629–1637.

[20] White, A.T., Philp, A., Fridolfsson, H.N., Schilling, J.M., Murphy, A.N., Hamilton, D.L., et al., 2014. High-fat diet-induced impairment of skeletal muscle insulin sensitivity is not prevented by SIRT1 overexpression. American Journal of Physiology — Endocrinology and Metabolism 307:E764—E772.

[21] Kim, H.J., Higashimori, T., Park, S.Y., Choi, H., Dong, J., Kim, Y.J., et al., 2004. Differential effects of interleukin-6 and -10 on skeletal muscle and liver insulin action in vivo. Diabetes 53:1060—1067.

[22] Glund, S., Deshmukh, A., Long, Y.C., Moller, T., Koistinen, H.A., Caidahl, K., et al., 2007. Interleukin-6 directly increases glucose metabolism in resting human skeletal muscle. Diabetes 56:1630—1637.

[23] Carey, A.L., Steinberg, G.R., Macaulay, S.L., Thomas, W.G., Holmes, A.G., Ramm, G., et al., 2006. Interleukin-6 increases insulin-stimulated glucose disposal in humans and glucose uptake and fatty acid oxidation in vitro via AMP-activated protein kinase. Diabetes 55:2688—2697.

[24] Moh, A., Zhang, W., Yu, S., Wang, J., Xu, X., Li, J., et al., 2008. STAT3 sensitizes insulin signaling by negatively regulating glycogen synthase kinase-3 beta. Diabetes 57:1227—1235.

[25] Jiang, L.Q., Duque-Guimaraes, D.E., Machado, U.F., Zierath, J.R., Krook, A., 2013. Altered response of skeletal muscle to IL-6 in type 2 diabetic patients. Diabetes 62:355—361.

[26] Ernst, M.B., Wunderlich, C.M., Hess, S., Paehler, M., Mesaros, A., Koralov, S.B., et al., 2009. Enhanced Stat3 activation in POMC neurons provokes negative feedback inhibition of leptin and insulin signaling in obesity. Journal of Neuroscience 29:11582—11593.

[27] Buettner, C., Pocai, A., Muse, E.D., Etgen, A.M., Myers Jr., M.G., Rossetti, L., 2006. Critical role of STAT3 in leptin's metabolic actions. Cell Metabolism 4: 49—60.

[28] Cernkovich, E.R., Deng, J., Bond, M.C., Combs, T.P., Harp, J.B., 2008. Adipose-specific disruption of signal transducer and activator of transcription 3 increases body weight and adiposity. Endocrinology 149:1581—1590.

[29] Bernier, M., Paul, R.K., Martin-Montalvo, A., Scheibye-Knudsen, M., Song, S., He, H.J., et al., 2011. Negative regulation of STAT3 protein-mediated cellular respiration by SIRT1 protein. Journal of Biological Chemistry 286:19270—19279.

[30] Phillips, D., Reilley, M.J., Aponte, A.M., Wang, G., Boja, E., Gucek, M., et al., 2010. Stoichiometry of STAT3 and mitochondrial proteins: implications for the regulation of oxidative phosphorylation by protein-protein interactions. Journal of Biological Chemistry 285:23532—23536.

[31] Wegrzyn, J., Potla, R., Chwae, Y.J., Sepuri, N.B., Zhang, Q., Koeck, T., et al., 2009. Function of mitochondrial Stat3 in cellular respiration. Science 323: 793—797.

[32] Szczepanek, K., Chen, Q., Larner, A.C., Lesnefsky, E.J., 2012. Cytoprotection by the modulation of mitochondrial electron transport chain: the emerging role of mitochondrial STAT3. Mitochondrion 12:180—189.

[33] Kim, J.H., Yoon, M.S., Chen, J., 2009. Signal transducer and activator of transcription 3 (STAT3) mediates amino acid inhibition of insulin signaling through serine 727 phosphorylation. Journal of Biological Chemistry 284: 35425—35432.

[34] Inoue, H., Ogawa, W., Asakawa, A., Okamoto, Y., Nishizawa, A., Matsumoto, M., et al., 2006. Role of hepatic STAT3 in brain-insulin action on hepatic glucose production. Cell Metabolism 3:267—275.

[35] Inoue, H., Ogawa, W., Ozaki, M., Haga, S., Matsumoto, M., Furukawa, K., et al., 2004. Role of STAT-3 in regulation of hepatic gluconeogenic genes and carbohydrate metabolism in vivo. Nature Medicine 10:168—174.

[36] Reilly, S.M., Ahmadian, M., Zamarron, B.F., Chang, L., Uhm, M., Poirier, B., et al., 2015. A subcutaneous adipose tissue-liver signalling axis controls hepatic gluconeogenesis. Nature Communications 6:6047.

[37] Cui, Y., Huang, L., Elefteriou, F., Yang, G., Shelton, J.M., Giles, J.E., et al., 2004. Essential role of STAT3 in body weight and glucose homeostasis. Molecular and Cellular Biology 24:258—269.

[38] Nguyen, M.T., Favelyukis, S., Nguyen, A.K., Reichart, D., Scott, P.A., Jenn, A., et al., 2007. A subpopulation of macrophages infiltrates hypertrophic adipose tissue and is activated by FFAS via TLR2, TLR4 and JNK-dependent pathways. Journal of Biological Chemistry 282:35279—35292.

